J|A|C|S
ARTICLES
Published on Web 05/01/2007

On the Mechanism of Peripentacene Formation from Pentacene: Computational Studies of a Prototype for Graphene Formation from Smaller Acenes

Brian H. Northrop, Joseph E. Norton, and K. N. Houk*

Contribution from the Department of Chemistry and Biochemistry, University of California, Los Angeles, California 90095

Received January 24, 2007; E-mail: houk@chem.ucla.edu

Abstract: The formation of peripentacene during the high-temperature vacuum sublimation of pentacene (**P**) in the presence of trace amounts of 6,13-dihydropentacene (**DHP**) has been studied computationally with density functional theory. Computational and kinetic analyses indicate that competing mechanisms involving a series of H atom transfers initiated by hydrogen transfer from **DHP** to **P** can account for the formation of peripentacene. The overall reaction is predicted to proceed with a free energy barrier of 36.1 kcal/mol and to be autocatalytic. Kinetic modeling supports the proposed mechanism.

Introduction

Pentacene has attracted enormous attention as an organic semiconductor.[1,2] In device applications such as organic thin film transistors (OTFTs),[3−8] pentacene has shown some of the highest charge carrier mobilities, 0.1−5.0 μ ($cm^2\ V^{-1}\ s^{-1}$), of all organic materials.[4,9] Fabrication and purification techniques have progressed sufficiently that carrier mobilities in pentacene-based OTFTs can rival even silicon-based transistors.[6,10−12] It is also well known, however, that the purity of pentacene and the quality of the crystal lattice in pentacene-based devices strongly influence carrier mobilities. Defects in the crystal lattice resulting from improper crystallization or chemical impurities may adversely affect performance.[12−18] Therefore, it is of great importance to be able to obtain highly pure samples of pentacene. A recent report by Roberson et al.[19] has demonstrated that sublimation of pentacene in the presence of trace amounts of 6,13-dihydropentacene (**DHP**) can lead to the formation of additional **DHP**, various disproportionation products, as well as the previously unknown peripentacene (Scheme 1a).[19] This simple procedure for the fusion of two polyacenes to give a larger graphene[20,21] fragment could be a general way to synthesize such species.

As noted by Roberson et al., HPLC/UV−vis spectral analysis and electron impact mass spectrometry (EIMS) showed that commercially available pentacene contains nonnegligible amounts of **DHP**, 6,13-pentacene quinone (**PQ**), Al, and Fe.[19] Purification of commercially available pentacene samples by vacuum sublimation at temperatures above 300 °C using a highly pure carrier gas resulted in the production of **DHP** along with additional residue. Analysis of the residue by laser desorption Fourier transform mass spectrometry (FTMS) revealed a mass peak at 546 *m*/*z* identified as the previously unknown peripentacene, which may be considered a nanographene.[20,21] The formation of polynuclear aromatics from smaller unsaturated hydrocarbons is not without precedent.[22,23] Lewis and Edstrom have studied the thermal reactivity characteristics of polyaromatic hydrocarbons (PAH) leading to carbonization of polynuclear aromatics.[22] More recently, Field et al. observed the production of graphitic species as well as hydrogenated aromatics from PAHs under high mechanical pressures.[23] Based

(1) Pope, M.; Swenberg, C. E. *Electronic Processes in Organic Crystals and Polymers*, 2nd ed.; Oxford University Press: Oxford, 1999; pp 337−340.
(2) Clar, E. *Polycyclic Hydrocarbons*; Academic Press: London, 1964.
(3) Garnier, F. *Chem. Phys.* **1998**, *227*, 253−262.
(4) Dimitrakopoulos, C. D.; Malenfant, P. R. L. *Adv. Mater.* **2002**, *14*, 99−117.
(5) Minari, T.; Nemoto, T.; Isoda, S. *J. Appl. Phys.* **2004**, *96*, 769−772.
(6) Horowitz, G. *J. Mater. Res.* **2004**, *19*, 1946−1962.
(7) Kato, Y.; Iba, S.; Teramoto, R.; Sekitani, T.; Someya, T.; Kawaguchi, H.; Sakurai, T. *Appl. Phys. Lett.* **2004**, *84*, 3789−3791.
(8) For recent reviews of organic thin film transistors see: (a) Katz, H. E. *J. Mater. Chem.* **1997**, *7*, 369−376. (b) Horowitz, G. *Adv. Mater.* **1998**, *10*, 365−377. (c) Katz, H. E.; Bao, Z. *J. Phys. Chem. B* **2000**, *104*, 671−678. (d) Katz, H. E.; Bao, Z.; Gilat, S. L. *Acc. Chem. Res.* **2001**, *34*, 359−369. (e) Ling, M. M.; Bao, Z. *Chem. Mater.* **2004**, *16*, 4824−4840. (f) Sun, Y.; Liu, Y.; Zhu, D. *J. Mater. Chem.* **2005**, *15*, 53−65. (g) Anthony, J. E. *Chem. Rev.* **2006**, *106*, 5028−5048.
(9) Shtein, M.; Mapel, J.; Benziger, J. B.; Forrest, S. R. *Appl. Phys. Lett.* **2002**, *81*, 268−270.
(10) Klauk, H.; Halik, M.; Zschieschang, U.; Schmid, G.; Radlik, W. *J. Appl. Phys.* **2002**, *92*, 5259−5263.
(11) Kelley, T. W.; Muyres, D. V.; Baude, P. F.; Smith, T. P.; Jones, T. D. *MRS Symp. Proc.* **2003**, *771*, 169.
(12) Bendikov, M.; Wudl, F.; Perepichka, D. F. *Chem. Rev.* **2004**, *104*, 4891−4945.
(13) Laquindanum, J. G.; Katz, H. E.; Lovinger, A. J.; Dodabalapur, A. *Chem. Mater.* **1996**, *8*, 2542−2544.
(14) Gundlach, D. J.; Lin, Y. Y.; Jackson, T. N.; Nelson, S. F.; Schlon, D. G. *IEEE Electron Device Lett.* **1997**, *18*, 87−89.
(15) Lin, Y.; Gundlach, D. J.; Nelson, S. F.; Jackson, T. N. *IEEE Trans. Electron Devices* **1997**, *44*, 1325−1331.
(16) Garnier, F. *Chem. Phys.* **1998**, *227*, 253−262.
(17) Fichou, D. *J. Mater. Chem.* **2000**, *10*, 571−588.
(18) Koch, N.; Ghijsen, J.; Johnson, R. L.; Schwarts, J.; Pireaux, J.-J.; Kahn, A. *J. Phys. Chem. B* **2002**, *106*, 4192−4196.
(19) Roberson, L. B.; Kowalik, J.; Tolbert, L. M.; Kloc, C.; Zeis, R.; Chi, X.; Fleming, R.; Wilkins, C. *J. Am. Chem. Soc.* **2005**, *127*, 3069−3075.
(20) Simpson, D. C.; Mattersteig, G.; Martin, K.; Gherghel, L.; Bauer, R. E.; Rader, H. J.; Müllen, K. *J. Am. Chem. Soc.* **2004**, *126*, 3139−3147.
(21) Wang, Z.; Tomovic, Z.; Kastler, M.; Pretsch, R.; Negri, F.; Enkelmann, V.; Müllen, K. *J. Am. Chem. Soc.* **2004**, *126*, 7794−7795.
(22) Lewis, I. C.; Edstrom, T. *J. Org. Chem.* **1963**, *28*, 2050−2057.
(23) Field, L. D.; Sternhell, S.; Wilton, H. V. *Tetraherdon* **1997**, *53*, 4051−4062.

10.1021/ja070392a CCC: $37.00

Scheme 1. (a) Experimentally Observed Formation of Peripentacene along with Additional 6,13-Dihydropentacene (**DHP**) during High-Temperature (>300 °C) Vacuum Sublimation of Pentacene in the Presence of Trace Amounts of (**DHP**); (b) Formation of 5,5′,6,6′-Di(phentacen-di-yl), a Precursor to Peripentacene, Studied Here Computationally

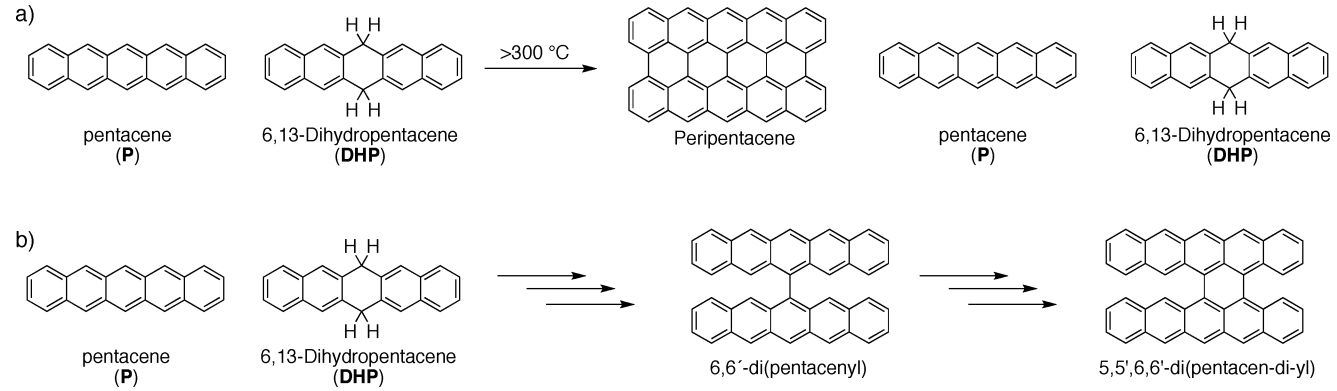

Scheme 2. Mechanism Proposed by Roberson et al. (ref 19) for the **DHP**-Catalyzed Peripentacene Formation during Sublimation of Pentacene at Temperatures Greater than 300 °C

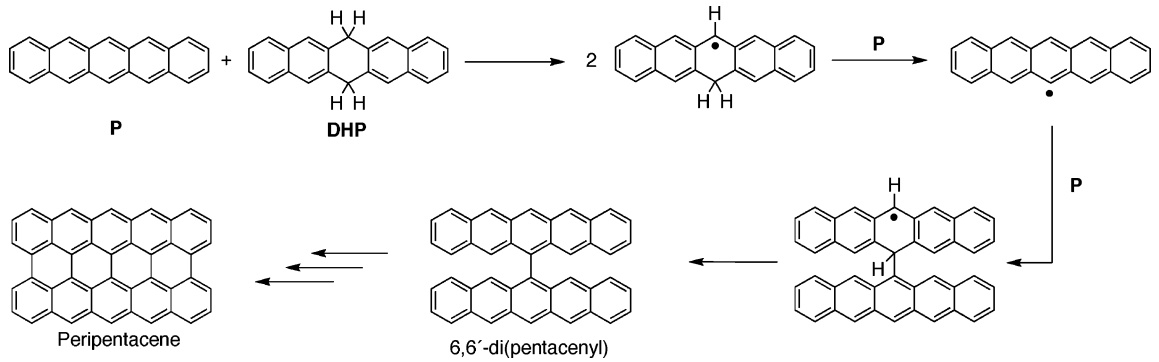

upon Rüchardt et al.'s studies of the H atom transfer reduction[24] of α-methylstyrene by 9,10-dihydroanthracene (**DHA**),[24,25] Roberson et al. proposed (Scheme 2) that the formation of peripentacene is catalyzed by **DHP**, which acts as a hydrogen donor in a manner similar to **DHA**.

We have carried out a theoretical study of the mechanism leading to the formation of **DHP** and 6,6′-di(pentacenyl), a precursor to the formation of peripentacene (Scheme 1b) that serves as a model for the steps leading to peripentacene formation, and have shown through computational and kinetic analysis that a series of H atom transfers originating from **DHP** explain the autocatalytic formation of peripentacene. The proposed mechanism differs from that of Roberson et al. in featuring addition of the 6-hydropentacenyl radical to pentacene, or dimerization of 2 equiv of the 6-hydropentacenyl radical, rather than hydrogen abstraction from pentacene.

Computational Details

Density functional theoretical (DFT) calculations were performed at the UB3LYP/6-31G* level[26] using the program Gaussian03.[27] Reaction free energies (ΔG°_{rxn}) were calculated for all steps of each proposed mechanism. Transition structures for hydrogen transfer processes were optimized at the UB3LYP/3-21G level and were distinguished from stationary points by having one imaginary vibrational frequency; energy minima have none. Vibrational and thermal analysis were used to obtain zero-point and thermal corrections of transition state free energies ($\Delta G^{\ddagger}$) in the gas phase at 1 atm and at 320 °C. Unrestricted wavefunctions were used for all radical and diradical species, while restricted and unrestricted wavefunctions gave identical results for closed-shell species.

Results and Discussion

The initial step of peripentacene formation involves hydrogen atom transfer from **DHP** to **P**, resulting in the formation of 2 equiv of 6-hydropentacenyl radical (**6PR**, Scheme 3). Roberson et al. proposed that **6PR** abstracts a hydrogen atom from pentacene resulting in the formation of a pentacenyl radical (**3**). A thorough exploration of this mechanism reveals that a key step, the abstraction of a hydrogen atom from pentacene, is a high-energy process and very unlikely. It is more likely, as will be demonstrated, that **6PR** will either dimerize or will add to pentacene. Dimerization and addition processes lead to the formation of tetrahydro and trihydro dipentacenyls, **1** and **2** (Scheme 3). Following the formation of these dipentacenyl derivatives, a series of hydrogen atom transfer steps leads to the formation of 6,6′-dipentacenyl, which is a precursor of peripentacene. A series of similar hydrogen atom transfer steps can complete the conversion of 6,6′-di(pentacenyl) to peripentacene. We have systematically explored how **1** and **2** can be converted to 6,6′-di(pentacenyl).

Potential Mechanistic Pathways. Transition states for hydrogen atom transfer and radical addition processes associated with the formation of **6PR** and **1**−**3** are shown in Scheme 4. H atom transfer from **DHP** to **P** (Scheme 4a), the initial step common to all mechanistic pathways, has a free energy barrier

(24) For a review of uncatalyzed transfer hydrogenation and transfer hydrogenolysis see: Rüchardt, C.; Gerst, M.; Edenhoch, J. *Angew. Chem., Int. Ed.* **1997**, *36*, 1406−1430.
(25) Morgenthaler, J.; Rüchardt, C. *Eur. J. Org. Chem.* **1999**, 2219−2230.
(26) Becke, A. D. *J. Chem. Phys.* **1993**, *98*, 5648−5652.
(27) Frisch, M. J.; et al. *Gaussian 03*, revision C.02; Gaussian, Inc.: Wallingford CT, 2004.

Scheme 3. Hydrogen Atom Transfer from **DHP** to **P** Results in the Formation of **6PR** which, through Either Dimerization or Addition to Pentacene, Produces Tetrahydro and Trihydro Dipentacenyls **1** and **2**[a]

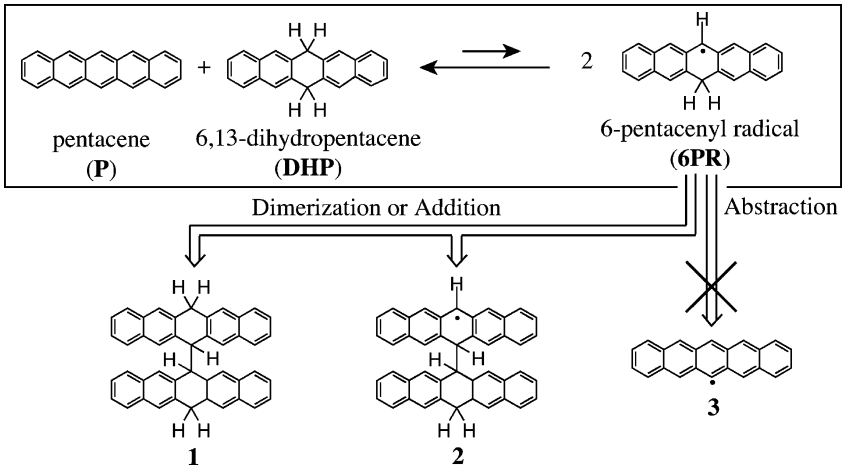

[a] Abstraction of a hydrogen atom from pentacene by **6PR** to form pentacenyl radical **3** is an unlikely, high-energy process.

Scheme 4. Transition States and Computed Reaction Activation Enthalpies ($\Delta H^{\ddagger}$) and Free Energies ($\Delta G^{\ddagger}$) for Hydrogen Atom Transfer from **DHP** to **P** (a), Hydrogen Abstraction from **P** (b), Addition of **6PR** to **P** (c), and Dimerization of **6PR** (d)[a]

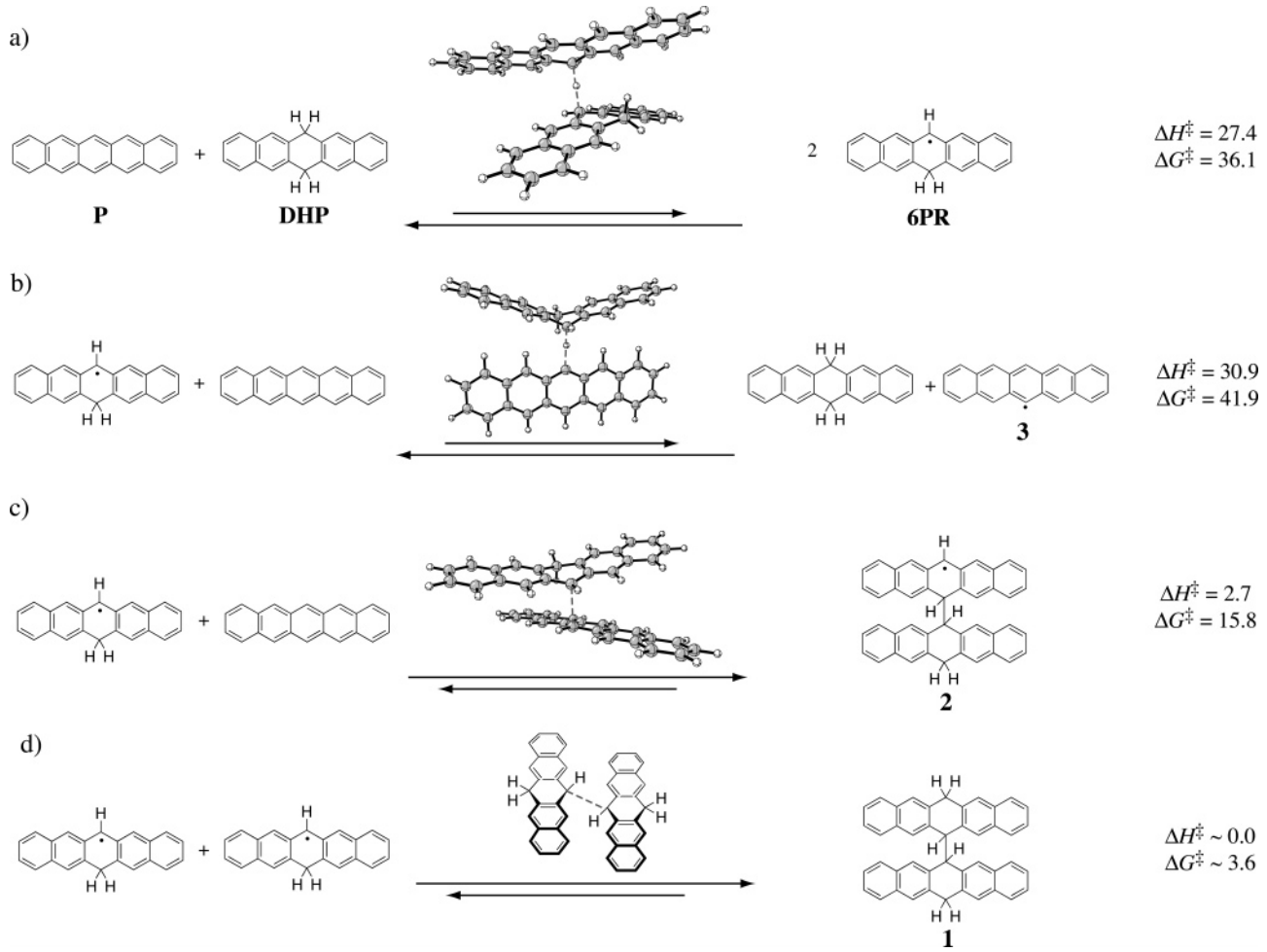

[a] Bonds being broken or formed are indicated by dashed green lines.

of 36.1 kcal/mol and is endothermic by 17.4 kcal/mol. The abstraction of a hydrogen atom from pentacene by **6PR**, as proposed by Roberson et al., requires 41.9 kcal/mol (Scheme 4b). Abstractions of aromatic hydrogens at the 4-, 5-, or 6-position have nearly the same activation energies and give radicals of nearly identical energies (Figure 1a). There should be no regioselectivity for this process. Mass spectral analysis by Roberson et al. indicates a preference for the formation of peripentacene consisting of aligned pentacene moieties (Scheme 1a) rather than misaligned "slip" isomers, though some evidence of small amounts of slip isomers does exist. The Roberson et al. mechanism should give a nearly statistical distribution of peripentacene slip isomers, in contrast to experimental observations.

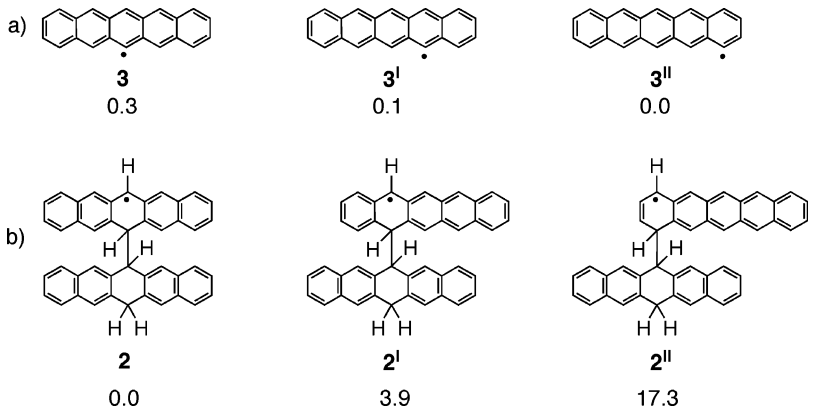

Figure 1. Relative energies (UB3LYP/6-31G*, kcal/mol) of isomers of radicals **2** and **3**.

Addition of **6PR** to pentacene (Scheme 4c) has a free energy barrier of only 15.8 kcal/mol, which is 26.1 kcal/mol lower than the previously discussed hydrogen abstraction barrier. As shown in Scheme 4, addition of **6PR** to **P** is highly favored to occur at the 6-position rather than the 4- or 5-positions; these adducts are 15.7 and 3.7 kcal/mol less stable, respectively (Figure 1b). These results are consistent with the experimentally observed preference for the formation of peripentacene with aligned pentacene moieties, resulting from further reactions of the favored adduct, **2**.

A transition state for dimerization of two **6PR** radicals (Scheme 4d) could not be located. However, dimerization is expected to have only a small entropic barrier with a free energy barrier similar to that of methyl radical combination, which occurs[28] with a rate constant of 2.40×10^{10} s^{-1}, corresponding to a free energy barrier of $\Delta G^{\ddagger} = 3.6$ kcal/mol. Dimerization is therefore expected to be 38.3 kcal/mol easier than abstraction, although the dimerization pathway is infrequent due to the low concentration of the radical, **6PR**, compared to **P** and **DHP**.

Having established that the formation of adducts **1** and **2** from **P** and **DHP** is preferred to formation of pentacenyl radical **3**, we explored the reactions of these hydrogenated pentacene dimers. The divergent mechanistic pathways leading from the formation of **6PR** and **2** to form tetrahydro and dihydro pentacene dimers **1** and **4** are shown in Scheme 5. The conversion of hydrogenated pentacene dimers **1** and **4** to 6,6′-di(pentacenyl) is achieved through a series of H atom transfer steps. For each H atom transfer step, either **P** or **6PR** may act as a H atom acceptor. Transition state free energies for H atom transfer processes occurring between either **P** or **6PR** and hydrogenated pentacene dimers **1**, **2**, and **4** are shown in Scheme 6 and were calculated using **6PR** and **DHP** as model systems for the analogous hydrogenated pentacene dimers. The possibility of H atom transfer between two dimeric pentacene derivatives was not considered given the low concentration of such derivatives relative to **P** and **6PR**. The formation of diradical species was also not considered as they are particularly high-energy species and unlikely to be formed.

Conversion of Hydrogenated Pentacene Dimers to 6,6′-Di(pentacenyl). The tetrahydro dipentacenyl, **1**, can be converted to **4** by two sequential H atom transfer steps to other hydrogen acceptors, either radical, **6PR**, or nonradical, **P**. Scheme 7 shows the eight possible routes for this overall dehydrogenation reaction. H atom abstraction from **1** can occur from either the 6- or 13-position, resulting in endo[29] radical species **5** or exo radical species **2**. In both cases, **P** or **6PR** may act as the H atom acceptor, resulting in four possible ways of generating a $C_{44}H_{29}^{\bullet}$ radical. The reaction is much easier with **6PR**, but **P** will be present in much higher concentration. Subsequent H atom abstraction from either of the two isomeric $C_{44}H_{29}^{\bullet}$ radicals (**5** and **2**) by either **P** or **6PR** gives the closed-shell species $C_{44}H_{28}$ (**4**).

A similar analysis can be applied (Scheme 8) to the conversion of dihydro pentacene dimer **4** to 6,6′-di(pentacenyl) (**8**). Again, **P** or **6PR** may act as a H atom acceptor to remove a hydrogen atom from **4** and generate either of the two isomeric $C_{44}H_{27}^{\bullet}$ radicals, **6** (exo) and **7** (endo). H atom abstraction from either of these two monohydro pentacene dimers results in the formation of 6,6′-di(pentacenyl) (**8**).

Analysis of Computed Reaction Free Energies and Free Energy Barriers. Overall, 144 possible mechanistic pathways[30] have been theoretically studied for the formation of 6,6′-di(pentacenyl) along pathways outlined in Schemes 5, 7, and 8. These pathways are summarized in Scheme 9. The contributions of each of these mechanisms to the formation of 6,6′-di(pentacenyl) are dependent upon the overall free energy barriers and concentrations of reactive species, especially of **P** and **6PR** involved in the bimolecular H atom transfer steps. Each mechanistic pathway is initiated by **DHP** (Scheme 9) and involves the consumption and production of **6PR**, which serves as a hydrogen atom transfer catalyst. Analysis of all mechanistic pathways reveals that each of the 144 possibilities can give overall reaction (1):

$$3\mathbf{P} \rightarrow \mathbf{8} + \mathbf{DHP} \qquad (1)$$

The rate-determining step will be shown to correspond to the initial reaction between **P** and **DHP**, which has a computed free energy barrier of 36.1 kcal/mol.

(28) An experimental study of the recombination kinetics of methyl radicals by molecular modulation spectrometry showed no observable temperature dependence. See: Parkes, D. A.; Paul, D. M.; Quinn, C. P. *J. Chem. Soc., Faraday Trans. 1* **1976**, *72*, 1935−1951.

(29) The terms exo and endo refer to the location of the radical that would be left behind (were it not in resonance) following the abstraction of a hydrogen from the 6- or 13-position, respectively, of a hydrogenated pentacene dimer such as **1**.

(30) The total number of potential mechanistic pathways was determined as follows: there are two possible routes for the formation of **1** (paths A or C in Scheme 5), eight possible routes for the conversion of **1** to **4** (paths E−L in Scheme 7), and eight possible routes for the conversion of **4** to **8** (paths M−U in Scheme 8) resulting in 128 different pathways for the formation of **1** and its conversion to **8**. Furthermore, **2** may be formed along paths B or D in Scheme 5, and then converted to **8** along any of the eight paths of Scheme 8 (M−U), resulting in 16 additional pathways for the formation of **8** for a total of 144.

Scheme 5. Initial Formation of **6PR** from Hydrogen Transfer between **P** and **DHP**, along with Dimerization and Addition Pathways Leading to the Formation of Dimeric Pentacene Derivatives **1**, **2**, and **4**[a]

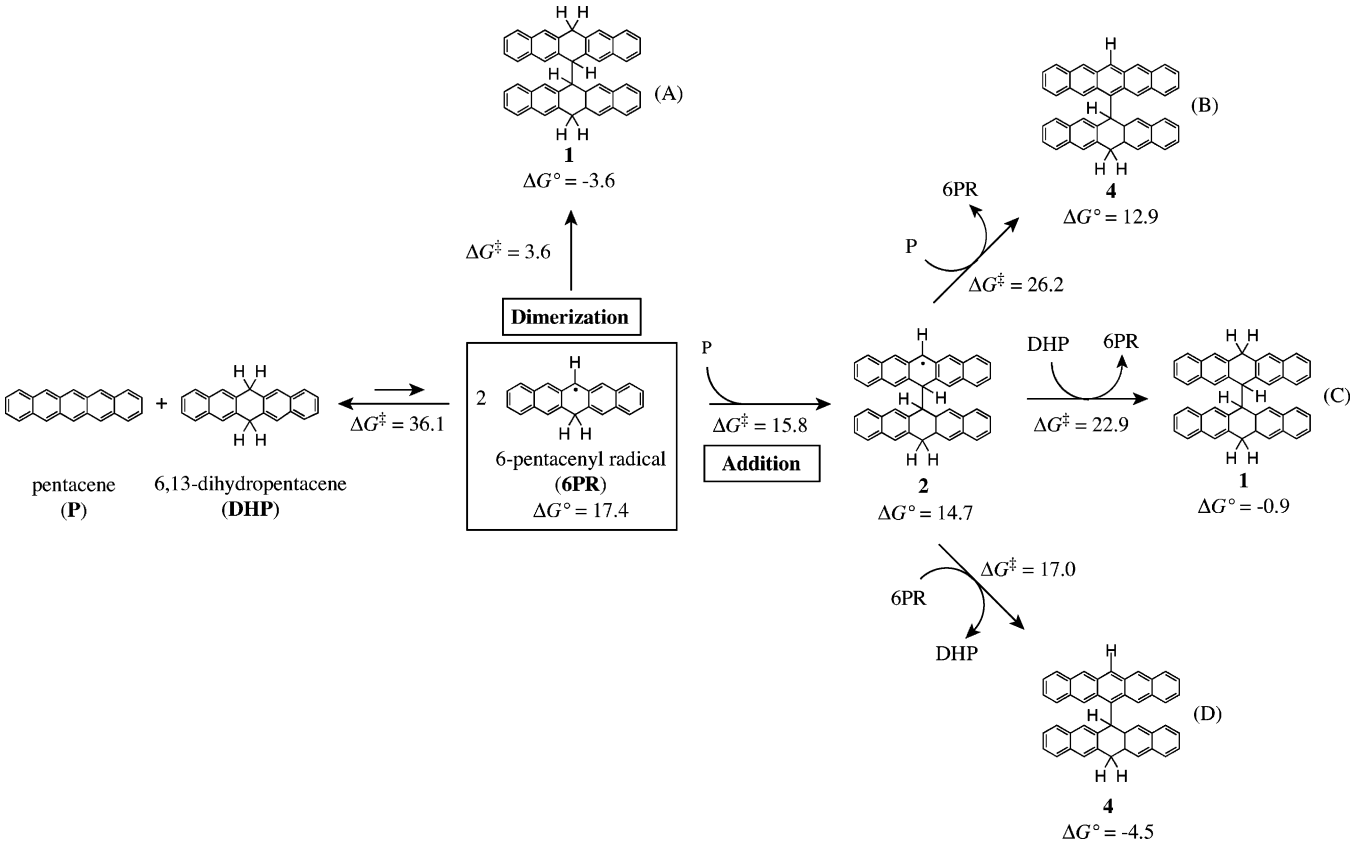

[a] Individual branching pathways have been labeled A−D for energetic and kinetic analysis. Free energy barriers ($\Delta G^{\ddagger}$) and reaction free energies (ΔG°_{rxn}), which have been calculated for each individual reaction, are given in kcal/mol.

Scheme 6. Transition States as Well as Reaction Activation Enthalpies ($\Delta H^{\ddagger}$) and Free Energies ($\Delta G^{\ddagger}$) for H Atom Transfer Processes Involving **P**, **6PR**, and **DHP**[a]

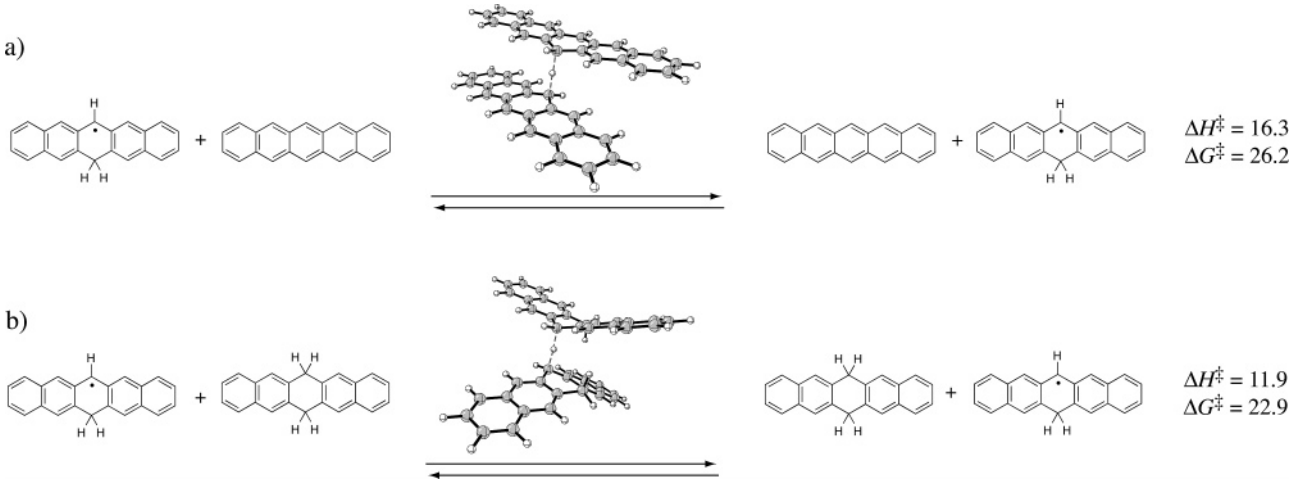

[a] Bonds being broken or formed are indicated by dashed green lines.

Kinetic Analysis. The reactions described here are related to Rüchardt's studies of the kinetics of H atom transfer from dihydroaromatics (e.g., **DHA**,[24,25] dihydronaphthalene,[24] xanthene,[31] etc.) to hydrogen acceptors (e.g., styrenes,[32] dienes,[33] imines,[34] etc.). Heating α-methylstyrene and an excess of **DHA** in diphenyl ether to 270−320 °C gave nearly quantitative production of cumene and anthracene.[24,25] The reaction has been shown to proceed by a stepwise radical mechanism (Figure 2) with an experimental free energy barrier of 44.1 kcal/mol involving two sequential hydrogen transfers from **DHA** to α-methylstyrene. The experimental vacuum sublimation temperatures resulting in the production of peripentacene from

(31) (a) Friebolin, H.; Rüchardt, C. *Liebigs Ann.* **1995**, 1339−1341. (b) Friebolin, H. Ph.D. Dissertation, University of Freiburg, 1997.
(32) Friebolin, H.; Roers, R.; Edenhoch, J.; Gerst, M.; Rüchardt, C. *Liebigs Ann.* **1997**, 385−389.
(33) Morgenthaler, J.; Rüchardt, C. *Liebigs Ann.* **1996**, 1529−1532.
(34) Morgenthaler, J. Ph.D. Dissertation, University of Freiburg, 1997.

Scheme 7. Eight Pathways that Have Been Explored for Conversion of **1** to **4** via Two Sequential H Atom Transfer Steps[a]

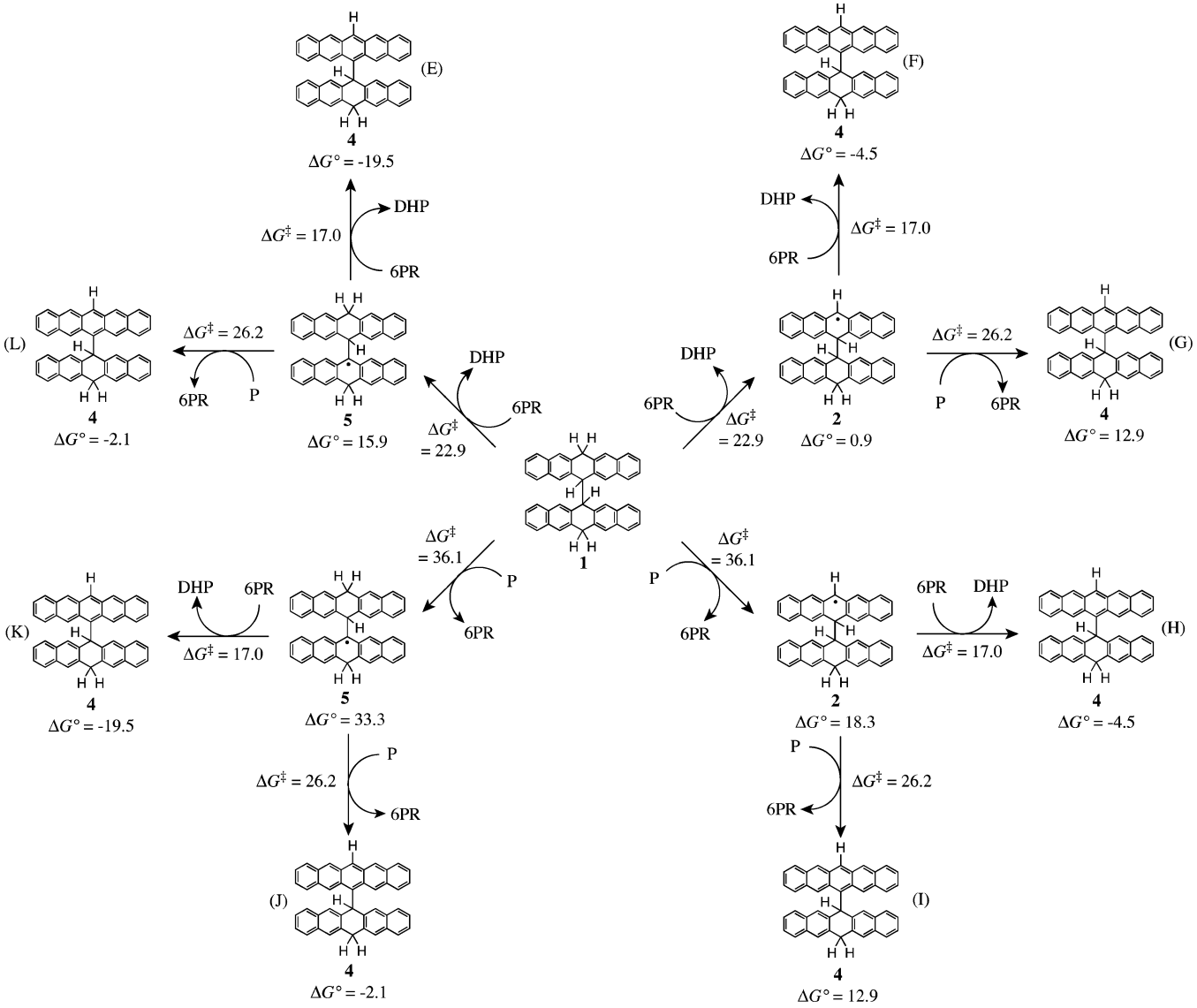

[a] Free energy barriers ($\Delta G^{\ddagger}$) and reaction free energies (ΔG°_{rxn}), which have been calculated for each individual reaction, are given in kcal/mol.

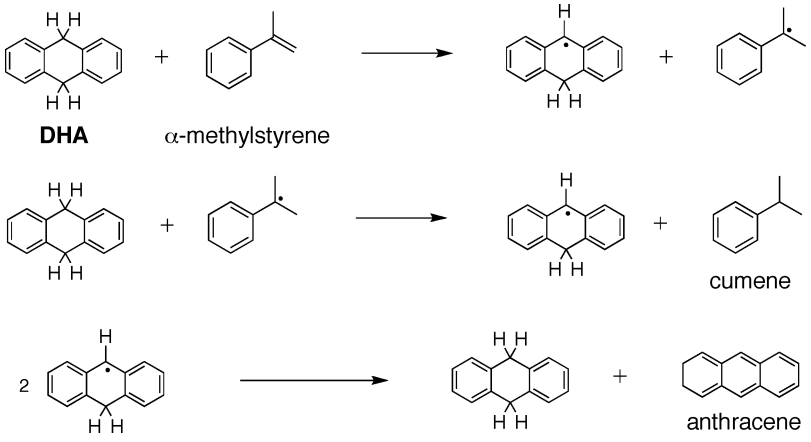

Figure 2. H atom transfer reduction of α-methylstyrene by 9,10-dihydroanthracene (**DHA**) to give cumene and anthracene.

pentacene are in the same range (~320 °C) as those necessary for H atom transfer from **DHA** to α-methylstyrene.

In the case under study, there are a great number of competing reactions. To evaluate the kinetics, the program Kintecus[35] was used to evaluate all of the 44 competing reactions[36] that give rise to the 144 routes that can be traced to form pentacene 6,6′-di(pentacenyl). This method of kinetic modeling allows for the rapid modeling of chemical kinetic processes given reaction rates

(35) Ianni, J. C. *Kintecus*, version 3.82, 2005, www.kintecus.com.

Scheme 8. Eight Pathways that Have Been Explored for Conversion of **4** to 6,6′-Di(pentacenyl) (**8**) via Two Sequential H Atom Transfer Steps[a]

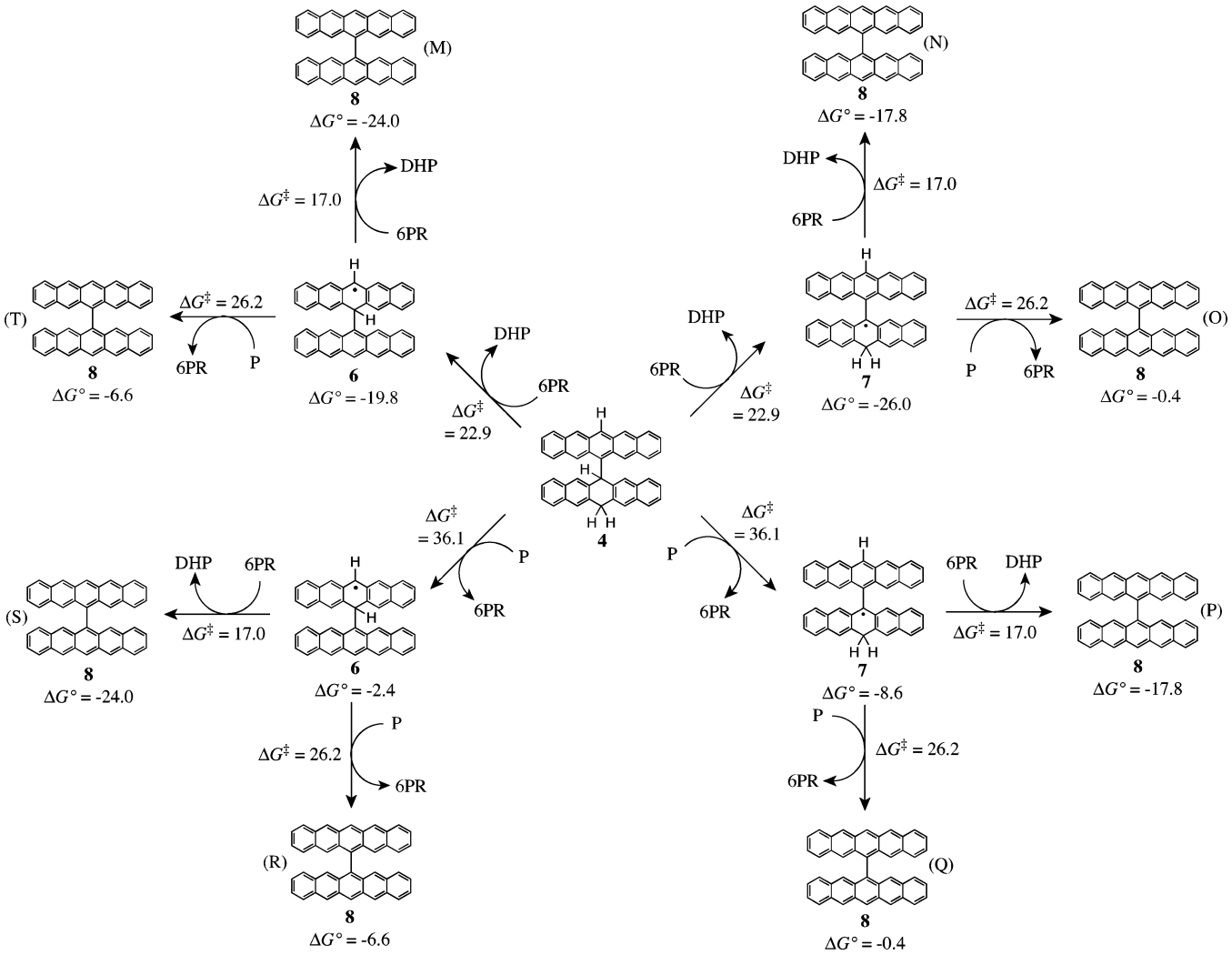

[a] Calculated free energy barriers ($\Delta G^{\ddagger}$) and reaction free energies (ΔG°_{rxn}) are listed for each individual step and given in kcal/mol.

and the initial concentrations of reactants. Rates of the forward and reverse reactions for every step of the 144 mechanistic pathways were determined from their calculated free energy barriers ($\Delta G^{\ddagger}$) using Eyring parameters at 320 °C. All reactions were considered to be reversible.

The concentration of solid pentacene is 4.27 M,[37] which was used as the initial pentacene concentration for all kinetic modeling. The initial concentration of **DHP** was arbitrarily chosen to be 0.2 M (5.7 mol %). The effect of varying the initial concentration of **DHP** from 0.0002 to 2.0 M (0.0005 to 33 mol %) was also considered. It is currently unclear whether the formation of peripentacene occurs in the gas phase or in the hot solid during the sublimation of pentacene in the presence of **DHP**. While molecules in the gas phase have more energy available for them to react, bimolecular reactions are more likely to occur in the hot solid where the concentration of molecules is greater. However, molecular motions are much more restricted in the hot solid than they are in the gas phase and it is less likely that molecules in the crystal are able to adopt the necessary transition state geometries. While it is likely that both possibilities contribute to the formation of peripentacene, the computational techniques and kinetic modeling employed in the current study were modeled in the gas phase at a temperature of 320 °C for a period of 4−24 h in accordance with the experimental conditions of Roberson et al.[19] The concentrations of pentacene, **DHP**, **6PR**, 6,6′-di(pentacenyl), and all intermediate species were evaluated as a function of time.

The forward and reverse reactions corresponding to each of the 144 mechanistic pathways were evaluated independently using the kinetic modeling program. The output of kinetic modeling, which gives the concentrations of **P**, **DHP**, **6PR**, and all dimeric pentacene derivatives as a function of time, was used to determine which of the pathways lead to 6,6′-di(pentacenyl) formation within 24 h of sublimation at 320 °C. Kinetic modeling reveals that 35 pathways result in the formation of appreciable quantities of 6,6′-di(pentacenyl) without the buildup of significant concentrations of intermediate products (see the

(36) Different combinations of 40 separate reactions (20 forward and 20 reverse) are able to account for each of the 144 pathways leading to the formation of 6,6′-di(pentacenyl). For completeness, the possibility of hydrogen abstraction from **P** by **6PR** and subsequent addition of **6PR** to **P**, as proposed by Roberson et al., was also taken into account in the kinetic modeling, as were the corresponding reverse reactions. A total of 44 reactions were, therefore, modeled simultaneously.

(37) Campbell, R. B.; Trotter, J.; Robertson, J. M. *Acta Crystallogr.* **1961**, *14*, 705.

Scheme 9. Summary of the 144 Reaction Pathways Studied Here Leading to the Formation of 6,6′-Di(pentacenyl)[a]

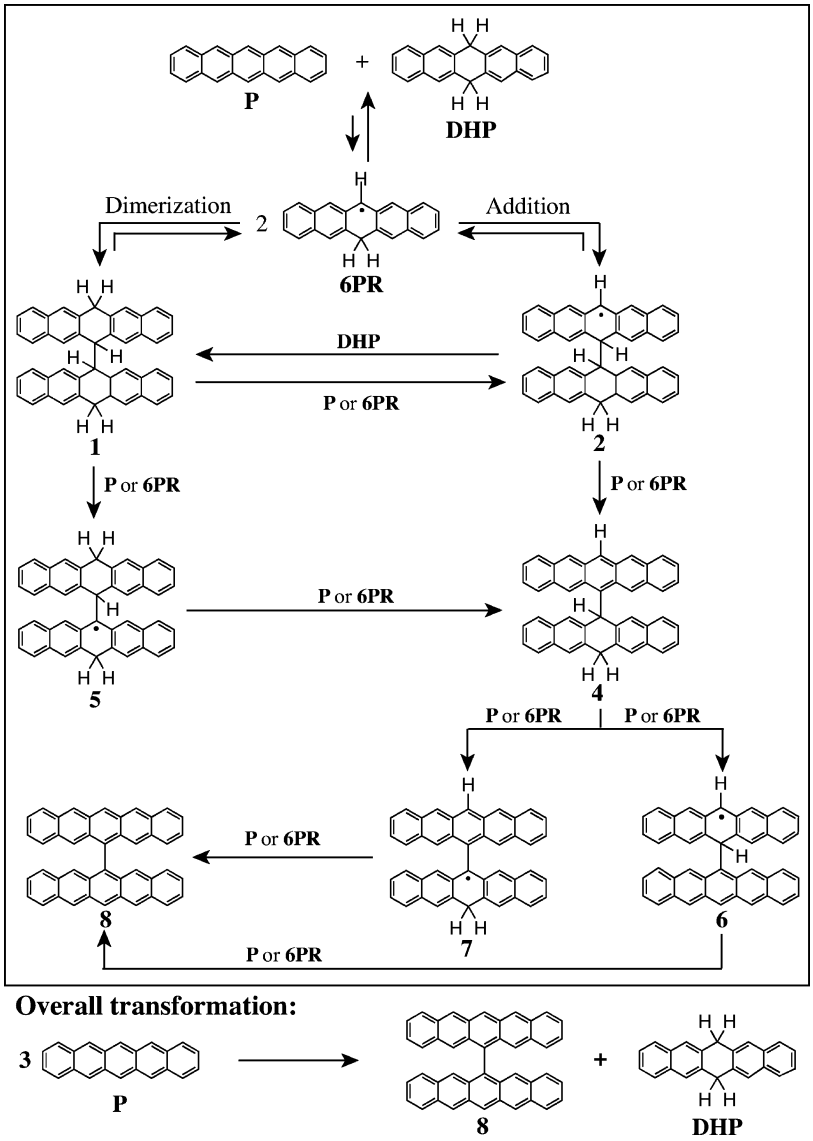

[a] All pathways are initiated by the reaction of **P** with **DHP** to give 2 equiv of **6PR**, which then either dimerizes or adds to another equivalent of **P** to form tetrahydro and trihydro dipentacenyls **1** and **2**, respectively. A series of intermolecular H atom transfer steps leads to the formation of 6,6′-di(pentacenyl) (**8**). H atom transfer occurs through reactions with **DHP**, **P**, or **6PR** as indicated above reaction arrows, producing either **6PR** or **DHP** (not shown) in each case. All mechanistic pathways transform 3 equiv of **P** to 1 equiv each of **8** and **DHP**.

Supporting Information). All 35 6,6′-di(pentacenyl)-producing pathways generate **DHP**.

The 35 mechanistic pathways that contribute to the formation of 6,6′-di(pentacenyl) (**8**) follow many of the same general reaction routes, and their similarities provide insight into the details of peripentacene production. Kinetic modeling reveals that **8** is formed only along mechanisms originating from pathways A and C and not from B or D. The formation of **8** along the dimerization pathway, A, is facilitated by the low free energy barrier ($\Delta G^{\ddagger} = 3.6$ kcal/mol) to dimerization of two **6PR** radicals. Pathways B, C, and D each involve the addition of **6PR** to **P** to form **2**, followed by reaction of **2** with **P**, **DHP**, or **6PR**, respectively. The reaction of **2** with **6PR** along pathway D has the lowest free energy barrier ($\Delta G^{\ddagger} = 17.0$ kcal/mol) and is exothermic by 4.5 kcal/mol, though this reaction will occur less frequently because of the low concentration of **6PR**. Pathway B, involving reaction of **2** with **P**, may occur frequently due to the high concentration of **P**. However, the reaction is endothermic by 12.9 kcal/mol and the reverse reaction will proceed faster than the forward one. In pathway C, **2** reacts with **DHP** with a free energy barrier that is 3.3 kcal/mol lower than for its reaction with **P** along pathway B, and the process is slightly exothermic. The relatively low free energy barrier, appreciable concentration of **DHP**, and reaction exothermicity favor pathway C over pathways B and D.

All kinetically viable pathways leading to the formation of **8** involve the formation of tetrahydrodipentacenyl derivative, **1**, since they all originate along pathways A or C. Following the formation of **1**, dehydration to form **8** may proceed along many of the competing reaction pathways shown in Schemes 7 and 8. Kinetic modeling provides a means for each of the individual competing reaction pathways to be evaluated and can revealed which reaction pathways do contribute to the formation of **8** and which do not. For example, kinetic modeling predicts that pathways E, G−I, and L of Scheme 7 and P of Scheme 8 do not contribute substantially to the formation of **8**.

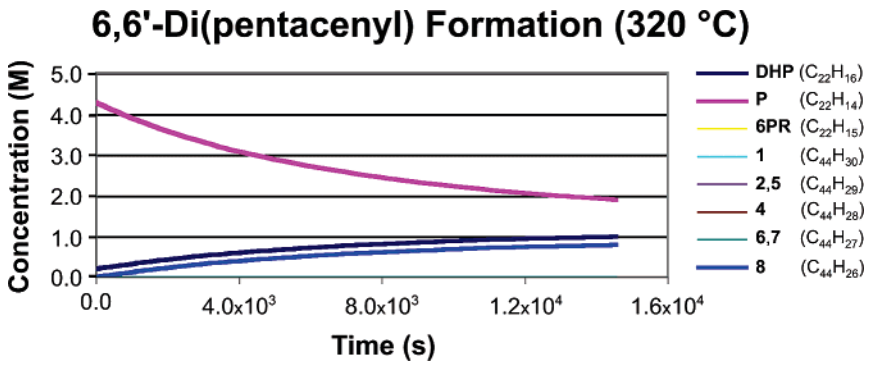

Figure 3. Output obtained from kinetic modeling, plotted as concentration (M) vs time (s), of the formation of 6,6′-di(pentacenyl) (**8**, $C_{44}H_{26}$) after 4 h of sublimation at 320 °C. The concentrations of species **6PR**, **1**, **2**, and **4**−**7** are all below 10^{-4} M and cannot be seen above the baseline.

Table 1. Comparison of the Quantity of 6,6′-Di(pentacenyl) Produced after 4 h of Sublimation as the Initial Concentration of **DHP** is Varied from 0.0002 to 2.0 M, as Well as when the Temperature is Lowered to 280 °C

DHP_0 (M)	temp (K)	6,6-di(pentacenyl) (M)
0.0002	593	0.669
0.002	593	0.688
0.02	593	0.709
0.2	593	0.773
2.0	593	0.813
0.2	553	0.021

Considering mechanistic pathways separately in this way, while helpful in determining which pathways contribute to the formation of 6,6′-di(pentacenyl), is insufficient to provide a complete description of the formation of 6,6′-di(pentacenyl) as competing reactions are not considered. A more accurate kinetic model is obtained when factoring in all 144 pathways simultaneously. The results of such analysis are shown in Figure 3 and indicate that, when all competing mechanistic pathways are considered, H atom transfer processes originating from retrodisproportionation of **P** and **DHP** can account for the autocatalytic production of 6,6′-di(pentacenyl), and presumably, peripentacene as well.

Kinetic modeling was also used to evaluate the effect of changing the initial concentration of **DHP**. Results of kinetic analysis with initial **DHP** concentrations of 0.0002, 0.002, 0.02, 0.2, and 2.0 M are shown in Table 1. As may be expected, lower initial concentrations of **DHP** result in less production of 6,6′-di(pentacenyl), while higher initial concentrations increase 6,6′-di(pentacenyl) production. However, the initial concentration of **DHP** does not affect the general outcome of the reaction, i.e., no other byproducts are formed. Kinetic modeling predicts that reducing the initial concentration of **DHP** from 2.0 down to 0.0002 M (0.01%) only decreases the amount of 6,6′-di(pentacenyl) produced by 17%. These results suggest that even as the initial concentration of **DHP** is reduced to trace amounts, it is still likely that peripentacene will be produced during the sublimation of pentacene at temperatures above 320 °C.

The effect of temperature on 6,6′-di(pentacenyl) production was also investigated (Table 1). Roberson et al.[19] noted that sublimation of pentacene at temperatures below 300 °C, even in the presence of **DHP**, did not result in the production of any peripentacene. Reaction rates at 280 °C were determined from computed free energy barriers using Eyring parameters and then input into the kinetic modeling program. In reasonable agreement with experimental observations, the production of is 6,6′-di(pentacenyl) is reduced 35-fold at this lower temperature (Figure 4).

Peripentacene Formation from 6,6′-Dipentacenyl. The computational and kinetic analysis thus far describes the formation of the central C−C bond of 6,6′-dipentacenyl. Indeed, no 6,6′-dipentacenyl is observed experimentally, so either an intermediate bypasses 6,6′-dipentacenyl altogether or 6,6′-dipentacenyl reacts faster than pentacene to eventually form peripentacene. Endo radicals **5** and **7** may, for example, undergo bond formation by an electrocyclic reaction prior to formation of 6,6′-dipentacenyl. The same process is not possible in the case of exo radicals **2** and **6**.

The formation of peripentacene from 6,6′-dipentacenyl by a mechanism strictly analogous to the formation of 6,6′-dipentacenyl (**8**) from pentacene is not likely because hydrogen atom transfer to 6,6′-pentacenyl from either **DHP** or **6PR** should occur mainly at the central carbon to regenerate **7** and **6PR** or **P**, respectively. Both hydrogen atom transfer processes are endothermic, with computed free energy barriers of 34.8 kcal/mol and 26.6 kcal/mol for hydrogen atom transfer from **DHP** or **6PR**, respectively. It would be more energetically favorable for **7** to bypass the formation of 6,6′-dipentacenyl altogether, as mentioned earlier, and undergo an electrocyclic ring closure (Scheme 10a) to form a second C−C bond and generate radical **10**. This unimolecular process has a computed free energy barrier[38] of 24.9 kcal/mol; however, the process is disfavored because ring closure is endothermic by 16.2 kcal/mol. Similarly, **5** may bypass the formation of 6,6′-dipentacenyl through a concerted electrocyclic ring-closing step that proceeds first from the abstraction of the endo hydrogen from **5** and then ring closure to form **13**, as shown in Scheme 10b. Formation of a second C−C bond along this electrocyclic ring closure pathway is disfavored by the relatively large free energy barrier[38] ($\Delta G^{\ddagger}$ = 42.0 kcal/mol) and reaction endothermicity of the electrocyclic ring closure step ($\Delta G°$ = 23.9 kcal/mol). Following the formation of **10** and **13**, a series of hydrogen atom abstractions would be required in order to form 5,5′,6,6′-dipentacen-di-yl (**16**). These bimolecular hydrogen atom abstraction steps are expected to be analogous to those that would have been required to transform **5** and **7** to 6,6′-dipentacenyl (**8**), and it is therefore believed that bypassing the formation of 6,6′-dipentacenyl through either endothermic electrocyclic ring closure process is not favored.

(38) Transition states for electrocyclic ring closure and direct coupling processes (Scheme 10a−d) were computed at the UB3LYP/3-21G level.

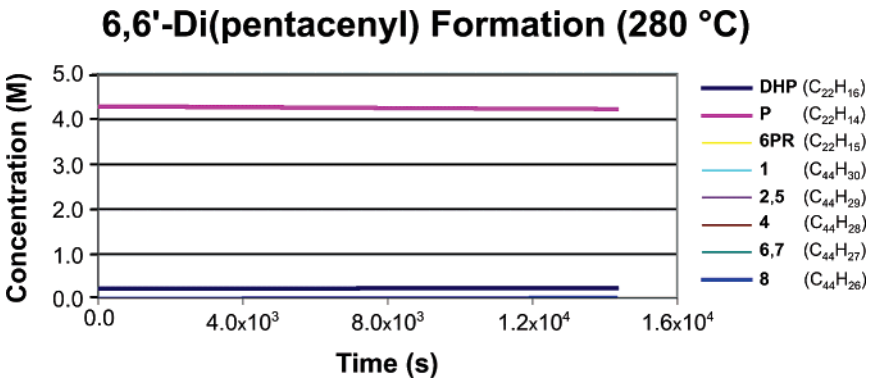

Figure 4. Results of kinetic modeling of the sublimation of **P** in the presence of 4.6 mol % **DHP** at 280 °C for 4 h. Modeling results are consistent with the experimental observation that peripentacene production is drastically reduced, if not completely stopped, at temperatures below 300 °C. The concentrations of species **6PR**, **1**, **2**, and **4**−**7** are all below 10^{-4} M and cannot be seen above the baseline.

Scheme 10. Mechanistic Pathways for the Formation of 5,5′,6,6′-Di(pentacen-di-yl) (**16**) that Have Been Explored Computationally[a]

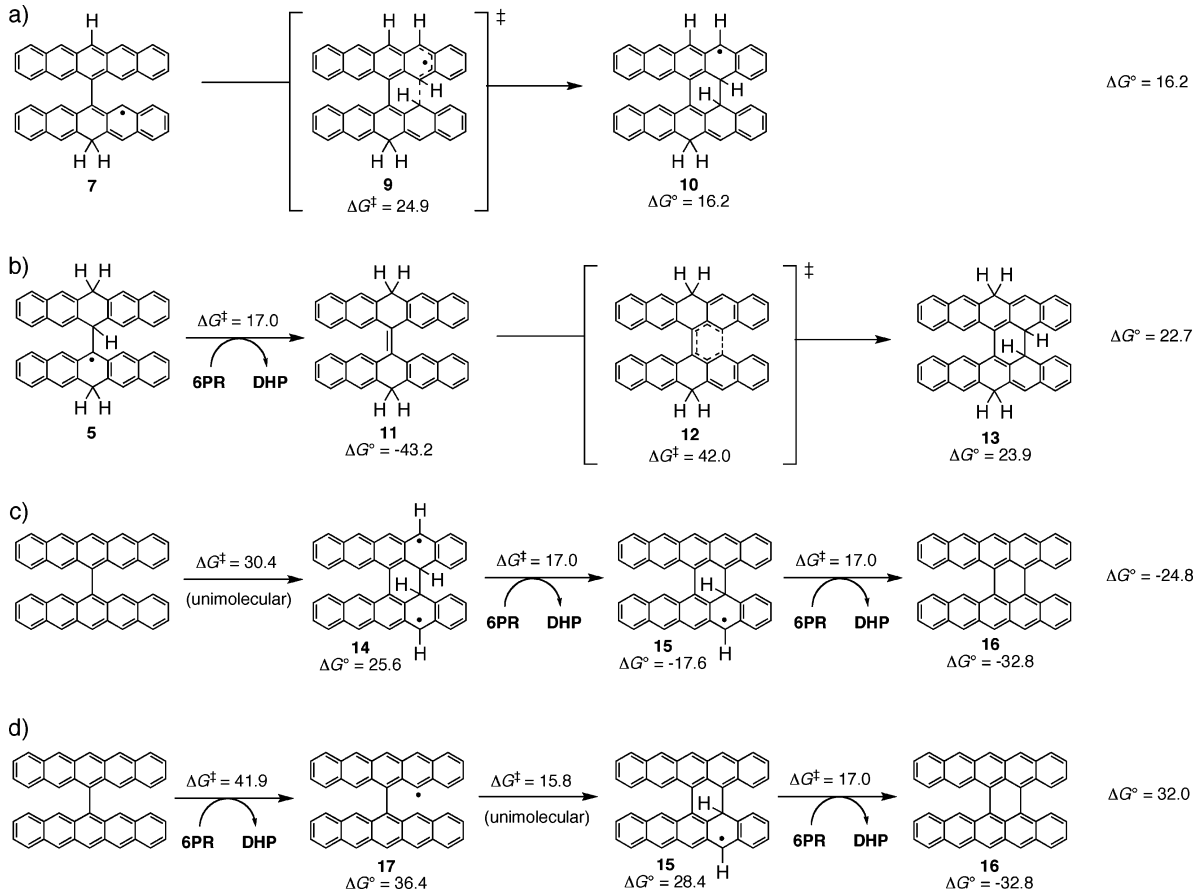

[a] Free energy barriers ($\Delta G^{\ddagger}$) and reaction free energies ($\Delta G°$) for each step are given in kcal/mol, as are the overall reaction free energies at the far right.

Two alternative pathways leading to the formation of a second C−C bond (5,5′,6,6′-dipentacen-di-yl, **11**) from 6,6′-dipentacenyl (**8**) have been studied computationally: direct coupling to form diradical **14** (Scheme 10c) and H atom abstraction from 6,6′-dipentacenyl followed by insertion (Scheme 10d). Reaction enthalpies and free energy barriers[38] have been computed for each of these processes and are shown in Scheme 10, parts c and d. Direct coupling of the upper and lower halves of 6,6′-di(pentacenyl) to form **14** has a free energy barrier of $\Delta G^{\ddagger} = 30.4$ kcal/mol. This unimolecular process will occur much faster than alternative bimolecular processes. Upon formation of diradical **14**, two sequential H atom transfers to **6PR** result in the formation of **16** with the overall process being exothermic ($\Delta G°_{rxn} = -24.8$). Hydrogen atom abstraction from 6,6′-dipentacenyl by **6PR** (Scheme 10d) requires 41.9 kcal/mol and is endothermic ($\Delta G°_{rxn} = 32.0$). Therefore, it is imagined that subsequent "zipping up"[19] of the upper and lower pentacene moieties continues through the direct addition pathway shown in Scheme 10c. A summary of the overall theoretically derived mechanism of peripentacene formation, which takes into account all dimeric pentacene derivatives that are likely formed as well as the subsequent formation of **16**, is shown in Scheme 11.

Scheme 11. Overall Summary of the Theoretically Derived Mechanism of Peripentacene Formation

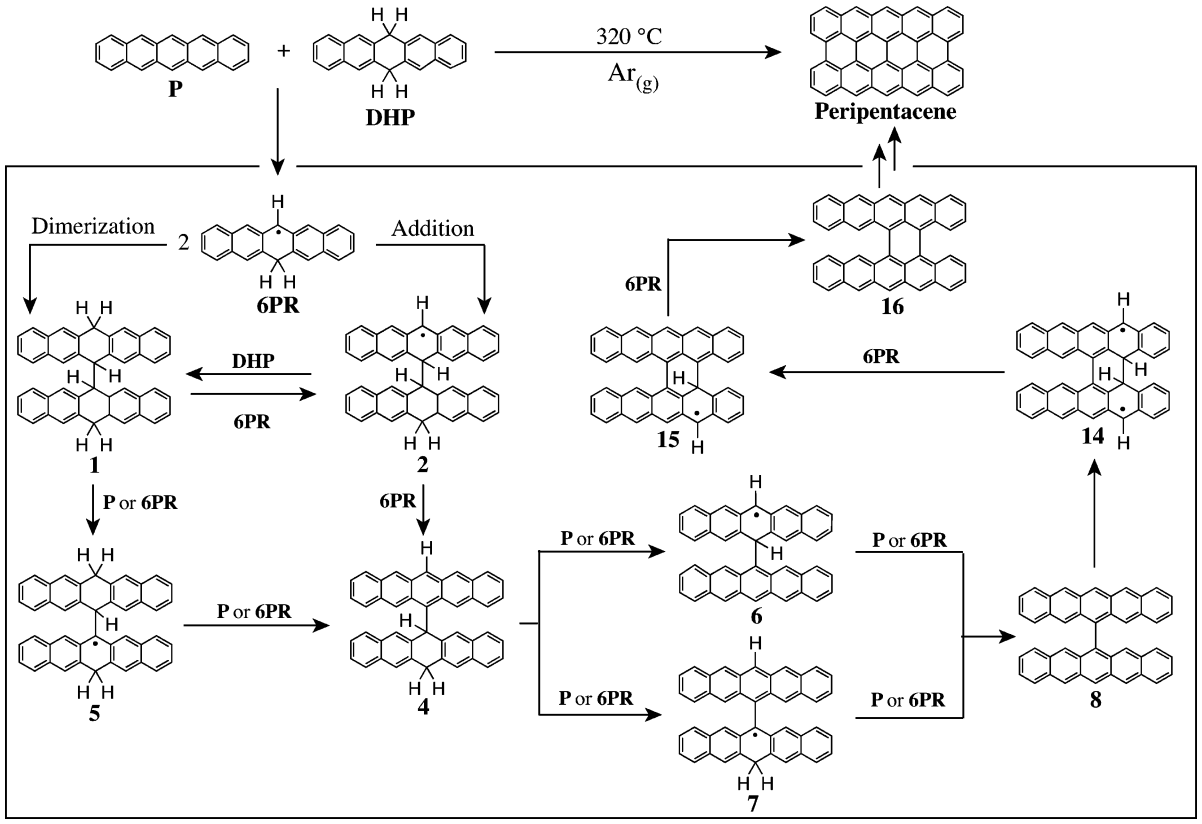

Conclusions

The potential mechanistic pathways for the initial stages in the formation of peripentacene and **DHP** during the high-temperature vacuum sublimation of commercially available pentacene have been modeled energetically and kinetically. The mechanism leading to 6,6′-dipentacenyl proceeds via H atom transfer from **DHP** to pentacene to form two **6PR** radicals, followed by dimerization or addition of **6PR** to **P** and subsequent aromatization by sequential H atom transfers. Only trace amounts of **DHP** are necessary to start this autocatalytic process. Kinetic analysis suggests that 35 of the 144 pathways studied are consistent with the experimental results of Roberson et al.,[19] and combined analysis of all 35 pathways suggests that they are in competition with each other in the formation of 6,6′-dipentacenyl. The rate-determining step for each of the mechanistic pathways corresponds to the initial H atom transfer from **DHP** to **P**, which has a computed free energy barrier of 36.1 kcal/mol. Following the formation of 6,6′-dipentacenyl, peripentacene is likely to be formed by a sequential series of coupling and intermolecular H atom transfer steps for each of the remaining six-membered rings. Such reactions are also relevant to the reactions of molecules with relatively weak C−H bonds and unsaturated hydrogen acceptors[24,25] such as the spontaneous polymerization of styrene,[39] disproportionation of **DHA** and 2-ethylanthracene,[40] the ane reaction,[41] transfer hydrogenation of ethane with cyclopentene,[42] and the formation of graphenes.[20,21]

Acknowledgment. We are grateful to the National Science Foundation for financial support of this research and to the ACS Division of Organic Chemistry for the Nelson J. Leonard ACS DOC Fellowship, sponsored by Organic Syntheses, Inc. to B.H.N. We thank the National Center for Supercomputing Applications and UCLA's Office of Academic Computing for computational resources.

Supporting Information Available: Cartesian coordinates for all optimized stationary points and transition states, computed reaction rates at 320 and 280 °C, summary of the concentrations of 6,6′-di(pentacenyl) produced along different reaction paths, and the full author list for ref 27. This material is available free of charge via the Internet at http://pubs.acs.org.

JA070392A

(39) (a) Chong, Y. K.; Rizzardo, E.; Solomon, D. H. *J. Am. Chem. Soc.* **1983**, *105*, 7761−7762. (b) Hall, H. K. *Angew. Chem., Int. Ed. Engl.* **1983**, *22*, 440−456. (c) Khuong, K. S.; Jones, W. H.; Pryor, W. A.; Houk, K. N. *J. Am. Chem. Soc.* **2005**, *127*, 1265−1277.
(40) (a) Stein, S. E. *Acc. Chem. Res.* **1991**, *24*, 350−356. (b) Camaioni, D. M.; Autrey, S. T.; Franz, J. A. *J. Phys. Chem.* **1993**, *97*, 5791−5792.
(41) (a) Metzger, J. O. *Angew. Chem., Int. Ed. Engl.* **1983**, *22*, 889−890. (b) Metzger, J. O.; Bangert, F. *Chem. Ber.* **1994**, *127*, 673−675.
(42) (a) Benson, S. W. *Int. J. Chem. Kinet.* **1980**, *XII*, 755−760. (b) *Thermochemical Kinetics*, 2nd ed.; John Wiley: New York, 1976. (c) Tsang, W. In *Energetics of Organic Free Radicals*, 1st ed.; Simões, J. A. M., Greenberg, A., Liebman, J. F., Eds.; Blackie Academic and Professional: London, 1996.